

DEVELOPMENT OF VIBROTACTILE SENSORY FEEDBACK FOR PROSTHETIC HAND USERS

Noor H.H. Mohamad Hanif, Paul H. Chappell, Neil M. White, Andy W. Cranny
Electronics & Computer Science, University of Southampton,
SO17 1BJ Southampton, United Kingdom.

nmh1r11@soton.ac.uk, phc@ecs.soton.ac.uk, nmw@ecs.soton.ac.uk, awc@ecs.soton.ac.uk

ABSTRACT

Executing daily chores with missing limbs is undoubtedly very challenging. For a person who has lost his lower arm, it is highly desirable to replace this loss with a device that not only identical in appearance, but closely mimics its capabilities. While there are many prosthetic products of multiple functionalities in the current market, the capability of the device to replicate the tactile sensory system are often neglected.

This research looks into supplementing a vibrotactile sensory feedback to the residual arm of prosthetic hand users. Surface information obtained at the fingertip of the prosthetic device becomes the input signals to the haptic actuator in generating vibration output. An Eccentric Rotation Mass (ERM) miniature motor has proven its capability to produce the required vibration in 2 dimensions within frequency bandwidth that matches the mechanoreceptor of the human skin. These findings are a stepping-stone in creating a real tactile sensation for prosthetic users.

KEY WORDS

Prosthetic, Bioinstrumentation, Vibrotactile, Sensory Feedback.

1. Introduction

When a person loses his lower arm, it hinders his capability to do simple tasks such as lifting, grasping, holding and touching, to name a few. With collaboration between medical practitioners and product developers, prosthetic devices are designed and fitted to the amputees depending on their needs. There are various types of upper limb prosthetic devices available in the market with varieties of functionality, sizes and appearance. The Michelangelo Hand by Ottobock, for instance, has capabilities of complex gripping kinematics and can move its fingers and thumb when cued by movement of arm stump [1], [2]. The Bebionic3 by RSL Steeper, on the other hand, is equipped with multiple grip positions and durable enough to lift objects up to 45 kg [3]. Another widely known prosthetic device product is i-Limb Ultra from Touch Bionics, that is capable of varying its grip strength according to necessities [4].

All three prosthetic devices are actuated by DC motors and battery powered. The Michelangelo Hand, for example, can be used up to 20 hours daily, and requires approximately 4 hours of charging time. This capability is very appealing as almost half of the population of the users wear their device more than 12 hours a day [5]. The grasp speed, depending on the size and shape of the object as well as the tasks required, plays a crucial role. It is suggested that 0.8-1.5 s grasping time is adequate for prosthetic hands [6].

However, although most of the functionalities have been replaced, these devices are mostly under-utilised or even rejected by the users [7]. Factors that lead to this abandonment includes user discomfort and extra time needed in manipulating the device [8]. Although the mass of the commercial prosthetic device is similar to that of the human hand, the sockets and their attachment have made the device heavier and less pleasant user experience [8]. There are also reported cases of mental stress when users have to rely on the visual or auditory cues when using the device [9].

Despite these drawbacks, devices equipped with sensory feedback capabilities have drawn great interest for the current and prospective users [7]. According to Raspopovic, to naturally mimic the capabilities of the lost hand as much as possible, the sensations perceived during object manipulation by the hand should also be present [10]. Many works have been focused on the mechanical movements of the hand, but the tactile sensing capabilities provided by the mechanoreceptors of the glabrous skin are often neglected.

The cutaneous mechanoreceptors in the human skin are responsible for human tactile sensations. Sensory endings in glabrous skin (skin that covers palm, sole of foot and the flexor surfaces of fingers and toes) are extremely sensitive to cutaneous stimulation. However only glabrous skin on the hand is used for tactile discrimination as the mechanoreceptors are located just beneath the skin layer [11]. People are able to distinguish the different roughness of a material with 5 μ m particles and the 9 μ m particles just by sliding their fingers on the material [12]. Depending on the sliding speed, angle between finger and material as well as the fingertip region, a fine surface with threshold as small as 2.2 μ m could be discriminated [13].

It is not until recently that the inclusion of sensory feedback into prosthetic devices is widely explored. A modified Ottobock prosthetic arm has been used to control the grasp force of a device using a haptic feedback simulator that incorporates vibrotactile (vibration sensory feedback) and visual cues [14]. In this research, the performance of the users to match the assigned grip force, improved tremendously when the vibrotactile responses were supplemented to the device. In another research, an artificial hand prosthesis (SmartHand) was designed to provide vibrotactile and mechanotactile (pressure / force sensory feedback) on amputees' residual arms [15]. Given a 0.36 N amplitude vibrations at 165 Hz, the task was to identify the locations of the stimulus between the five fingers. It was reported that it was harder to discriminate the vibrotactile stimuli as compared to the mechanotactile stimuli.

In works by Jamali and Sammut, different surface textures were distinguished via changes in frequencies detected by the silicone artificial finger embedded with Polyvinylidene Fluoride (PVDF) films [16]. The research hand developed by [17] employed the vibrotactile sensory modality to recognize and categorize different types of surface textures. Accuracies up to 80% were reported when multiple exploratory scratching behaviours were done on the test surfaces.

One of the research objectives at the Southampton University is to reproduce tactile sensation when a prosthetic finger slides across a surface texture. The reproduced tactile sensation will be felt at the residual arm. Various tactile sensations were investigated to select the best modality match between the fingertip and the arm. The Eccentric Rotation Mass (ERM) miniature DC motor has been identified to deliver the required vibrotactile sensation within the specified frequency bandwidths. Experiments were carried out to measure the amplitude of vibration generated by the motor. Adjustments of voltage inputs and other external factors were considered in achieving the optimum vibration amplitude. The experimental results were also compared with simulated results to validate their capabilities in providing reliable vibrotactile sensation to the upper arm.

2. Selection of Haptic Actuators

Haptic actuators are devices that are designed to recreate the kinaesthetic or tactile sensation. Kinaesthetic sensations are generated by activating the receptors within the muscles, joints and tendons while tactile sensations are generated through the activation of mechanoreceptors in the human skin [18]. As this research looks at discriminating surface textures, an emphasis will be placed on activating the sensory nerves on the human skin. These nerves are fired via various interactions on the skin such as friction, skin stretch, normal indentation, vibration, heat, shear, electrocutaneous and suction pressure [19].

In selecting a suitable haptic actuator, the physiological properties of the skin where the actuator to be mounted should be first understood. The skin that covers the upper arm is called hairy skin, which is less sensitive to vibration or pressure. However, at higher vibration frequencies, the skin sensitivity are similar to that of the glabrous skin [20]. This is contributed by the capability of the Pacinian corpuscles that could be activated by vibration frequencies as high as 400 Hz. A person could detect as low as 1 μ m of indentation on skin at about 250Hz, with the aid of the Pacinian corpuscles that could be fired within the particular frequency band [21].

2.1 Vibration Actuators

As the focus of the work is on recreating tactile sensations in deciphering surface texture, the vibration actuator is the best candidate as vibration is responsible in detecting the properties of a surface texture. At the right frequency and velocity, the vibrations felt at the fingertips during its sliding motion make it possible for texture discrimination. As it is better to have a modality match to achieve intuitive haptic feedback [22], it is desirable to process, recreate and amplify the vibration sensation felt at the fingertips so that the vibrations will also be felt at the residual arm. Furthermore, this stimulation is more suitable to discriminate rough or smooth sensations, if it is not at all painful and could be manipulated to be within the acceptable intensity band to avoid nerve or tissue damages.

With varying vibrations in terms of strength, frequency and pattern, the haptic actuators are very capable in providing users valuable tactile information. This mechanism is widely applied in mobile phones and pagers, to alert the users on incoming calls or messages. This mechanism is also commonly included in joysticks, to imitate the virtual sensation during video gaming sessions.

There are various models of haptic actuators currently available in the market. For this research purpose, the eccentric rotating mass actuator (ERM) has been selected as its advantages outweigh its limitations. An ERM vibration motor is a DC motor with an asymmetric mass attached to the shaft. As the ERM rotates, the centripetal force of the eccentric mass drives a net centrifugal force that leads to movement of the motor from its initial position. Repeated rotations of the ERM create a constant displacement of the motor, and are considered as vibration [23].

Table 1 summarizes the advantages and limitations of an Eccentric Rotation Mass (ERM).

Table 1: The advantages and limitations of Eccentric Rotation Mass (ERM) miniature DC motor

Advantages	Frequency bandwidth is within 0.1 to 300 HZ in which 250 Hz is the optimum frequency for the activation of Pacinian corpuscle located at the skin of the upper arm
	Low voltage requirement (3V rated voltage) which is highly desirable as it will be mounted onto human arm
	Low power consumption (typical 150 mW)
	Overall response time is recorded at 70 ms, which is adequate for typical tasks for prosthetic hands
	Generates vibrations in two axes (X and Z) which could be felt as stretching and indentation on the skin
	Low cost
Limitation	Slowest response as compared to other commercial actuators
	Produces noise due to vibration

The 304-111 Pico-Vibe™ 5mm vibration motor from Precision Microdrives has been identified as the best candidate to produce the required vibrotactile feedback. This actuator is chosen based on its response time, frequency bandwidth, low voltage requirement, low power consumption and low cost. The rated speed of the motor is 15 000 rpm (1570.8 rad/s) that is equivalent to 250 Hz of frequency. The voltage is rated at 3V with typical power consumption of 150 mW. The body diameter and length is 4.6 mm and 11 mm respectively with a unit mass of 1.1 g [24].

The miniature motor will be located at the upper arm although the spine or navel would have a greater vibrotactile sensitivity [25]. This is mainly because since it is the hand that lost the sensation, hence the sensory information should be supplemented to the hand. It is also preferable to choose the residual arm as it is nearer to the prosthetic device, hence shorter wiring. Furthermore, the ERM is capable of producing vibration that is within the detection threshold of the upper arm.

3. Simulation of the Vibrotactile Sensation

The transfer function of the motor has been identified to predict the vibration output of the system. The methodology and outcome of the MATLAB simulation have been previously published by Hanif [26]. By adjusting the input voltage, the driving frequencies generated by the motor is between 42 Hz to 251 Hz, which is in accordance to the frequency band of the mechanoreceptor at the hairy skin. The input voltage exhibits linear relationship with the motor speed and its linear frequency, as shown in Figure 1.

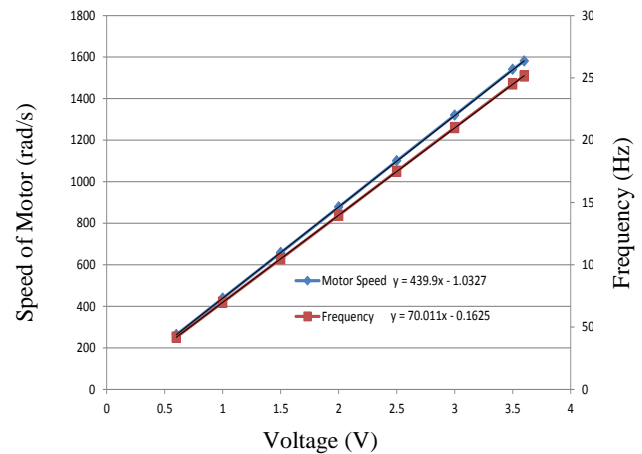


Figure 1: Speed of Motor (rad/s) and Frequency (Hz) vs. Voltage (V)

The relationships between the voltage versus the displacement and acceleration have also been explored, as shown in Figure 2. The displacement amplitude linearly increased with increment of voltage input as expected. The behaviour of the acceleration in relation to the voltage input is quadratic (second order) is also as predicted. This is because acceleration is a second order derivative of the displacement. The only parameters that remain almost constant throughout the voltage variation are the transient responses that include the settling time, rise time, natural frequency and the damping ratio.

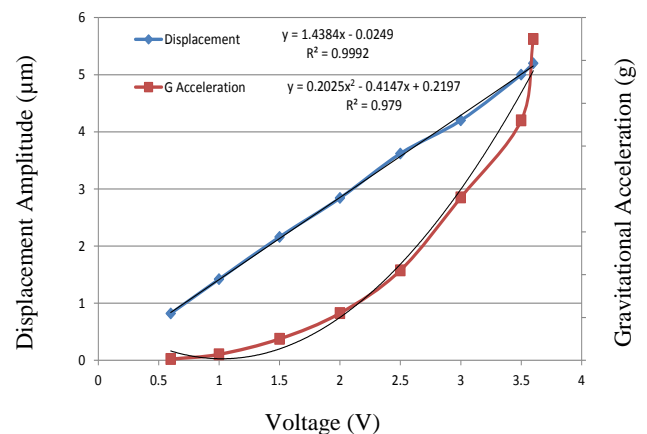


Figure 2: Displacement Amplitude (µm) and Gravitational Acceleration (g) vs. Voltage (V)

4. Measuring the Amplitude of Vibration

To validate the MATLAB simulation results, an experiment has been designed to measure the amplitude of vibration generated by the miniature DC motor. The LIS3L02AS4 linear accelerometer was selected to perform the task.

4.1 Hardware Configuration of LIS3L02AS4 Linear Accelerometer

A linear accelerometer is a sensor that provides a voltage output proportional to the detected gravitational acceleration and acceleration due to movement [27]. The LIS3L02AS4 linear accelerometer is a tri-axis (X, Y and Z directions) accelerometer with an IC interface that is able to acquire acceleration information and provide its analog signal to external devices such as oscilloscope or host computer. The range could be set at 2g or 6g according to its applications. The frequency bandwidths are 4 kHz for X, Y axes and 2.5kHz for Z axis [28].

To obtain best results with the accelerometer output, the frequency bandwidth should be the smallest possible for a given application. The maximum frequency of vibration generated by the miniature DC motor is 250 Hz, hence the cut-off frequencies (f_c) of the accelerometer outputs were chosen at 1 kHz. The cut-off frequencies were implemented by adding external capacitors ($C_{load(X,Y,Z)}$) at the output pins. These act as low pass filters for anti-aliasing and noise reduction for the circuit.

4.2 Calibration of LIS3L02AS4 Linear Accelerometer

To ensure the accelerometer is working in perfect condition, several characteristics of the accelerometer were tested against the manufacturers' datasheet. The characteristics include Zero-g level and Orientation.

4.2.1 Zero-g Level

The zero-g level corresponds to the output signal of the accelerometer without the presence of gravitational acceleration. On a horizontal surface, with the accelerometer pins pointing upwards, the sensor will measure zero-g in X and Y axes while +1g for Z axis. The accelerometer is factory calibrated at $V_{dd} = 3.3V$, hence the ideal voltage output, V_{out} , at zero-g is mid-way between 0 and 3.3V, i.e. $V_{out} = V_{dd}/2 = 1.650 V$. A deviation greater than the V_{out} is considered as positive acceleration, while deviation lesser than V_{out} is considered as negative acceleration. These deviations from the zero-g level are known as zero-g offset [27], [28].

For this application, the zero-g level of the accelerometer has been tested on a horizontal surface with the pins pointing downwards. The obtained voltage outputs will be considered in calibrating the accelerometer according to its orientation.

4.2.2 Orientation Check

The orientation check is important to relate the acceleration with the obtained output voltage. The output voltage are measured at 6 orientations of the accelerometer (+X, -X, +Y, -Y, +Z, -Z). These voltages correspond to the g acceleration at the chosen scale ($\pm 6g$). By tilting the accelerometer by 90° about the three axes,

any two of the readings would be 0g and the third would be either -3g or +3g.

A spirit level was used to ensure measurements were carried out at a level surface. To ensure a perfect 90° orientation, a protractor was placed on top of the scale, and the accelerometer was taped onto it.

By supplying an input voltage, V_{dd} of 3.3V to the accelerometer, the output voltages at every orientation were measured. These values are important in obtaining the linear relationship between the output voltage and its corresponding acceleration.

4.3 Experimental Apparatus for Vibration Measurement

The miniature motor is securely positioned on top of the accelerometer to record the generated vibration when voltage is supplied to it. As a common practice, a $100 \mu F$ (non-polar ceramic) decoupling capacitor was included with the motor circuit design. The motor is allowed to freely rotate and measurements were taken when the motor has reached steady-state. Two separate power sources were utilized to supply input voltages to the motor and accelerometer. Output data were measured using a 4-channel digital oscilloscope (Tektronix DPO3014). The outputs were recorded as V_{outx} , V_{outy} and V_{outz} , that represents voltage at X, Y and Z axes. The experimental setup and the accelerometer/ motor circuit are as shown in Figures 3 and 4 respectively.

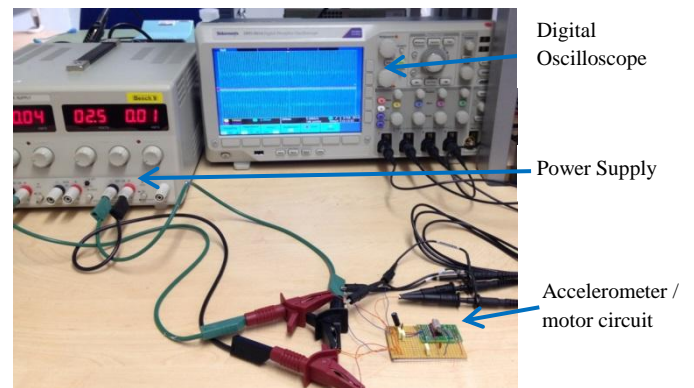


Figure 3: Experimental apparatus to obtain the vibration amplitude of the motor

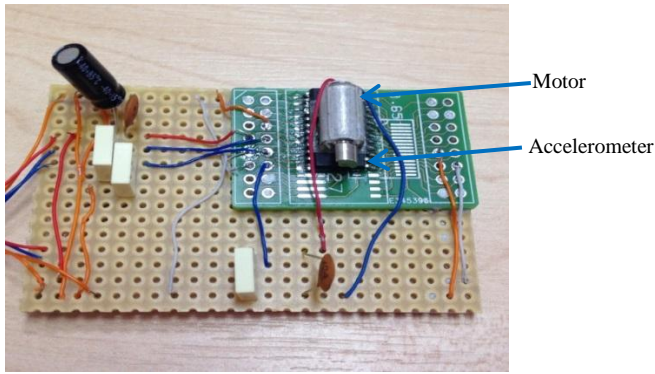


Figure 4: Accelerometer / motor circuit

5. Experimental Results

5.1 Acceleration Output

The acceleration outputs were recorded in the X, Y and Z axes at given input voltage to the motor. The input voltages were varied from the 0.6V (typical start voltage) and increased at 0.5V step size to 3V (rated voltage). Figure 5 shows the accelerations observed at the rated voltage 3V.

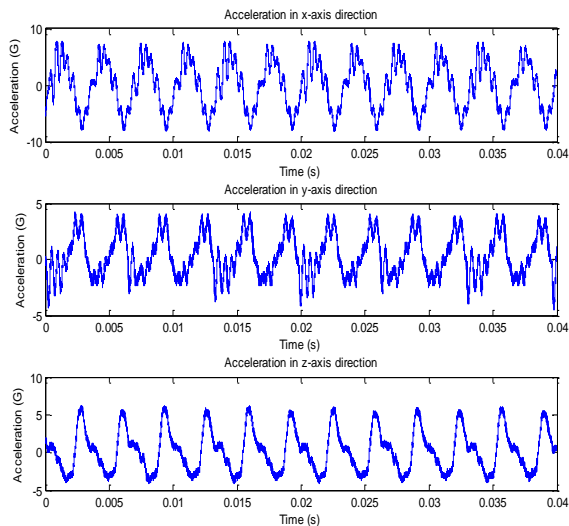


Figure 5: 3V supply – Acceleration in X, Y and Z axes

5.2 Frequency Response

The Fast Fourier Transform (FFT) was used to examine the frequency response generated by the motor vibration. Similarly, the input voltages were varied from the 0.6V (typical start voltage) and increased at 0.5V step size to 3V (rated voltage) and 3.6V (maximum operating voltage of the motor). Figure 6 shows the frequency response observed at the rated voltage 3V.

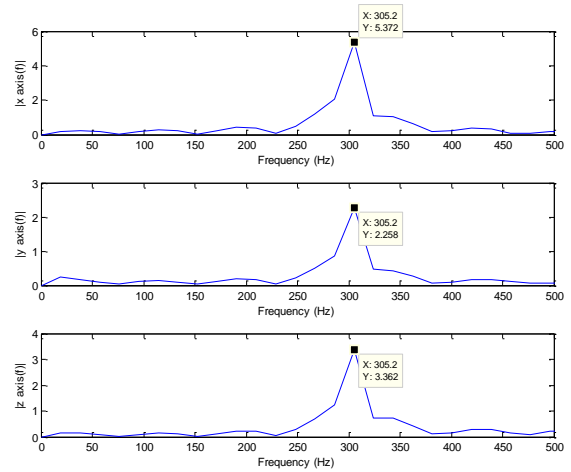


Figure 6: Frequency response observed for 3V in the X, Y and Z axes

5.3 Vibration Amplitudes and Frequency Response vs. Voltage Input of the Motor

Figure 7 shows the relationship between vibration amplitudes (in root mean square), with the motor input voltage while Figure 8 highlights the relationship of generated frequencies to the motor input voltage.

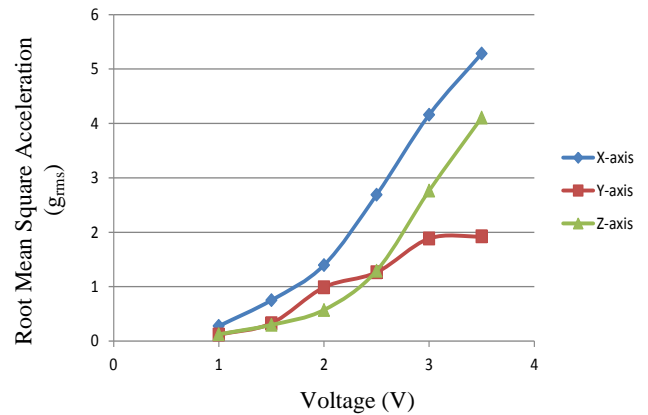


Figure 7: Acceleration (g) vs. Voltage (V)

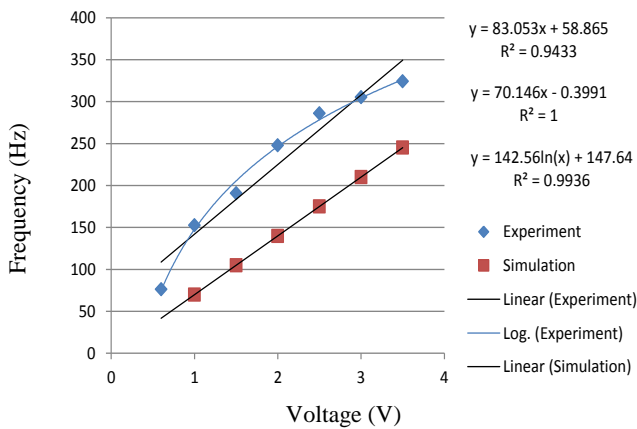


Figure 8: Vibration Frequency (Hz) vs. Voltage (V)

5.4 Discussions

From the experiment, the motor is struggling to rotate at 0.6V (Figure 7) with the highest peak acceleration recorded at 0.5g. As the voltage supply increases, the peak-to-peak acceleration of the motor picks up and goes beyond 16g peak-to-peak at 3V, which is much higher than the simulated results (Figure 2). This is because the mass of the circuit board tremendously affects the vibration amplitude. It would take less input supply to generate vibration for a lighter test rig and vice-versa [24]. The simulated results were based a 100 g test sled (manufacturer's datasheet) while the circuit board has a mass of 16.11 g. This finding is useful in adjusting the necessary circuitry mass of the haptic actuator to provide sufficient vibration to the skin.

For a given voltage supply, the motor will vibrate in two planes that are perpendicular to the body length of the motor [24]. For this application, the X and Z axes are perpendicular to the body length of the motor. It could be observed from Figure that the vibration experienced in the X and Z axes are much stronger as compared to the Y axis. When positioned on the skin surface, the vibrations in the X and Z axes will be felt as a slight stretching and indentation on the skin respectively.

To measure the effective vibration energy content, the measured peak-to-peak accelerations were converted to the root mean square (RMS) accelerations. The outcome of the conversion is as shown in Figure . It can be seen that the highest effective vibration content is recorded at 4.1g_{rms} at the X-axis with voltage supply of 3.5V. The plot is useful as it gives information on the actual vibration to be felt by the users at varying voltage inputs.

The relationship between the frequency and voltage supply for both simulation and experiment is plotted in Figure 8. By adding the linear trend lines to the plot, it was observed that the experiment result ($R^2=0.9433$) is not as perfectly linear as compared to the simulations results ($R^2=1$). This result is expected, as the motor is subjected to external factors during experiment, such as the way it is mounted and the actual maximum

frequency/vibration it could handle. Nevertheless the simulation results obtained previously provides a background idea on the behaviour the motor at different voltage supplies.

To further assess the relationship of the frequency of vibration to input voltage, a log trend line has been used. With the R^2 value of 0.9936, it gives reliable information in estimating the required voltage for a desired frequency of vibration.

It could be observed from Figure 8 that the motor generates vibration frequency between 76 Hz to 320 Hz depending on the input voltage. This frequency band falls within the frequency sensitivity of the hairy skin which is between 65 to 400 Hz [29]. The frequency of interest, which is 250 Hz, occurs when the motor is supplied with 2V. At this voltage, the gravitational accelerations (RMS) of the motor are 1.4g and 0.6g at the X and Z axes respectively.

To verify the capability of the chosen haptic actuator (the ERM motor) in providing vibration sensation to the residual arm, a psychophysics investigation will be conducted. As the haptic sensations shall correlate to the properties of the surface texture, the vibration will also be varied accordingly. The vibration effects from the on-off pulses as well as constant voltage supply will be tested to the volunteers, and their perception on the varying degrees of roughness and smoothness sensations will be evaluated.

6. Conclusion

This research work looks at reproducing the tactile sensation gathered by the prosthetic finger to be deciphered by users via vibration felt at the residual limb. In achieving this objective, it is important to determine and consequently manipulate the links between the tactile sensation and the haptic feedback.

Results from the MATLAB simulations show that the selected haptic actuator exhibits linear relationship between the input voltage and its driving frequency. Through the relationship, the vibration produced by the haptic actuator could be efficiently predicted. The quadratic behaviour between the input voltage and the acceleration suggests that the optimum input voltage range, in ensuring sufficient vibrotactile sensation, should be between 2V to 3.5 V. The transient responses obtained via the simulation also provide some estimation in preparing the next haptic event, such as the time it may take to decrease the amplitude of vibration.

The experimental results show the expected logarithmic relationship between the frequency and voltage. Through adjustments of input voltage, frequencies could be generated between 76 Hz to 320 Hz, which is within the frequency bandwidth of the sensitive mechanoreceptors in the human hairy skin. The optimum frequency of 250 Hz can be achieved with a 2 V input. At this frequency, the effective vibration energy in the X and

Z axes are 1.4 g_{rms} and 0.6 g_{rms} respectively, which are within the vibration detection threshold of the human hairy skin.

The findings from this research work have paved a way in providing valuable tactile sensations for upper limb prosthetic users. Volunteers will be sought to test the generated vibrotactile sensations and their feedback will be analysed in the later stage of this project.

References

- [1] "Fascinated. With Michelangelo," 2011. [Online]. Available: <http://www.living-with-michelangelo.com/gb/technology/#/2/1>.
- [2] C. Bates, "The bionic man: Victim of jet-ski accident becomes first person in UK to be fitted with pioneering limb," *Mail Online*, 23-Jan-2013.
- [3] "BeBionics3 Product Brochure," *RSLSteeper*, 2012. [Online]. Available: http://bebionic.com/distributor/documents/bebionics3_Product_Brochure.pdf. [Accessed: 31-Dec-2012].
- [4] "i-limb ultra," *Touch Bionics*, 2011. [Online]. Available: <http://www.touchbionics.com/media/2210/i-limb-ultra-data-sheet-lo-res.pdf>.
- [5] P. Kyberd and C. Wartenberg, "Survey of Upper-Extremity Prosthesis Users in Sweden and the United Kingdom," *JPO J. Prosthetics Orthot.*, vol. 19, no. 2, pp. 55–62, 2007.
- [6] R. Vinet, Y. Lozac'h, N. Beaudry, and G. Drouin, "Design methodology for a multifunctional hand prosthesis," *J. Rehabil. Res. Dev.*, vol. 32, no. 4, pp. 316–24, Nov. 1995.
- [7] E. A. Biddiss and T. T. Chau, "Upper limb prosthesis use and abandonment: a survey of the last 25 years," *Prosthet. Orthot. Int.*, vol. 31, no. 3, pp. 236–57, Sep. 2007.
- [8] J. T. Belter and A. M. Dollar, "Performance characteristics of anthropomorphic prosthetic hands," *IEEE Int. Conf. Rehabil. Robot. [proceedings]*, vol. 2011, p. 5975476, Jan. 2011.
- [9] J. Gonzalez, H. Soma, M. Sekine, and W. Yu, "Psycho-physiological assessment of a prosthetic hand sensory feedback system based on an auditory display: a preliminary study," *J. Neuroeng. Rehabil.*, vol. 9, p. 33, Jan. 2012.
- [10] S. Raspopovic and M. Capogrosso, "Restoring Natural Sensory Feedback in Real-Time Bidirectional Hand Prostheses," *Sci. Transl. Med.*, vol. 6, no. 222, 2014.
- [11] T. Pritchard and K. Alloway, Eds., *Medical neuroscience*, 1st ed. Connecticut: Hayes Barton Press, 1998, pp. 205–228.
- [12] T. Mano and M. Ohka, "Mechanisms of fine-surface-texture discrimination in human," *J. Acoust. Soc. Am.*, vol. 105, no. 4, pp. 2485–2492, 1999.
- [13] T. Kawamura, K. Tani, and H. Yamada, *Measurement System of Fine Step-Height Discrimination Capability of Human Finger's Tactile Sense*. InTech, 2012, pp. 163–178.
- [14] A. Chatterjee, P. Chaubey, J. Martin, and N. Thakor, "Testing a Prosthetic Haptic Feedback Simulator With an Interactive Force Matching Task," *JPO J. Prosthetics Orthot.*, vol. 20, no. 2, pp. 27–34, Apr. 2008.
- [15] C. Antfolk, M. D'Alonzo, M. Controzzi, G. Lundborg, B. Rosén, F. Sebelius, and C. Cipriani, "Artificial redirection of sensation from prosthetic fingers to the phantom hand map on transradial amputees: vibrotactile versus mechanotactile sensory feedback," *IEEE Trans. Neural Syst. Rehabil. Eng.*, vol. 21, no. 1, pp. 112–20, Jan. 2013.
- [16] N. Jamali and C. Sammut, "Material classification by tactile sensing using surface textures," in *2010 IEEE International Conference on Robotics and Automation*, 2010, pp. 2336–2341.
- [17] J. Sinapov, S. Member, V. Sukhoy, R. Sahai, and A. Stoytchev, "Vibrotactile Recognition and Categorization of Surfaces by a Humanoid Robot," *IEEE Trans. Robot.*, vol. 27, no. 3, pp. 488–497, 2011.
- [18] R. S. Dahiya, G. Metta, M. Valle, and G. Sandini, "Tactile Sensing—From Humans to Humanoids," *IEEE Trans. Robot.*, vol. 26, no. 1, pp. 1–20, Feb. 2010.
- [19] J. Pasquero, "Survey on communication through touch," Montreal, Canada, 2006.
- [20] J. Raisamo, "Tactile Sensing & Feedback," *pervasive.jku.at*, pp. 1–62, 2009.
- [21] E. Kandel, J. Schwartz, and T. Jessell, *Principles of neural science*, 4th ed., no. 1. McGraw Hill, 2000, pp. 432–451.
- [22] K. Kim and J. Colgate, "On the design of miniature haptic devices for upper extremity prosthetics," *IEEE/ASME Trans. Mechatronics*, vol. 15, no. 1, pp. 27–39, 2010.
- [23] "AB-004-Understanding ERM Vibration Motor Characteristics," *Precision Microdrives TM*, 2012. [Online]. Available: <http://www.precisionmicrodrives.com/application-notes-technical-guides/application-bulletins/ab-004-understanding-erm-characteristics-for-vibration-applications>. [Accessed: 24-Aug-2012].
- [24] "Pico Vibe™ Model: 304-111," vol. 44, no. 0. Precision Microdrives, pp. 1–7, 2013.
- [25] L. Jones and N. Sarter, "Tactile displays: Guidance for their design and application," *Hum. Factors J. Hum. Factors Ergon.*, vol. 50, no. 1, pp. 90–111, 2008.
- [26] N. H. H. M. Hanif, P. H. Chappell, A. Cranny, and N. M. White, "Vibratory feedback for

artificial hands,” in *2013 International Conference on Electronics, Computer and Computation (ICECCO)*, 2013, pp. 247–250.

- [27] H. Vathsangam, “Augmentative Communication Device,” 2010.
- [28] “MEMS INERTIAL SENSOR : 3Axis - 2g/6g Linear Accelerometer,” no. December. ST Microelectronics, pp. 1–14, 2005.
- [29] J. C. Makous, R. M. Friedman, and C. J. Vierck, “A critical band filter in touch.,” *J. Neurosci.*, vol. 15, no. 4, pp. 2808–18, Apr. 1995.